

Generation of Polarization-Entangled Twin Photons by Type-II QPM Waveguide NLO Device

Toshiaki Suhara, Hiroaki Okabe and Masatoshi Fujimura

Department of Electrical, Electronic and Information Engineering, Graduate School of Engineering,
Osaka University suhara@eei.eng.osaka-u.ac.jp

Abstract: A cross-polarized twin photon generation device was implemented with Ti-indiffused LiNbO₃ waveguides and domain-inverted gratings for Type-II (TE→TE+TM) quasi-phase matching. Generation of polarization-entangled twin-photon beams by a simple system using the fabricated device is demonstrated through quantum interference and photon polarization measurement experiments.

Introduction

There has been increasing research interest in quasi-phase-matched (QPM) waveguide nonlinear-optic (NLO) devices for applications to quantum information processing¹⁻⁶. An important element for quantum information technique is twin photons including photons of quantum entangled states, which offer a variety of possibilities such as quantum teleportation, quantum cryptography and quantum interface⁷. The authors are working on theoretical^{8,9} and experimental^{10,11} studies of waveguide QPM-NLO twin photon generation devices. Recently, we demonstrated implementation of a waveguide cross-polarized twin photon generation device based upon the Type-II QPM in a LiNbO₃ waveguide¹¹. Cross-polarized twin photons can easily be split into each photon by a polarization beam splitter without loss and spurious photon.

In this paper, we demonstrate generation of polarization entangled states by the Type-II QPM waveguide NLO device, and report the results of quantum interference experiments.

Type-II QPM waveguide NLO device

The Type-II QPM waveguide twin photon generation device configuration is shown in Fig.1. The device consists of a channel waveguide and a ferroelectric domain-inverted grating for QPM in a z-cut LiNbO₃ crystal. Twin photon generation is based on parametric fluorescence due to the NLO tensor element $d_{24}(=d_{31})$, and the phase matching is accomplished by the Type-II (TE→TE+TM) QPM. As annealed proton-exchanged waveguides often used for NLO devices support the extraordinary mode only, a Ti-indiffused waveguide capable of guiding both polarization modes was adopted in this work. Devices of the interaction length $L=30\text{mm}$ and the QPM grating periods around $\Lambda=9.2\mu\text{m}$ were fabricated for generation of (nearly-) wavelength-degenerate twin photons in the $1.55\mu\text{m}$ band.

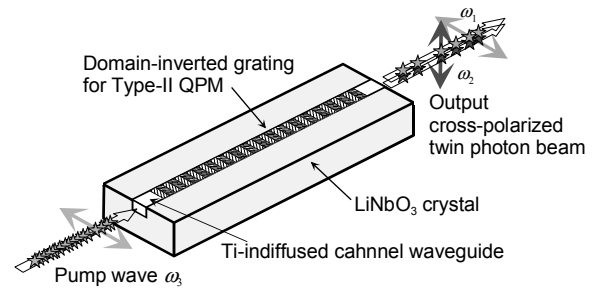


Fig. 1: Configuration of Type-II QPM waveguide NLO cross-polarized twin photon generation device.

The fabrication process was presented in detail in ref.11. At first Ti film of thickness~100nm of stripe pattern with $7.0\mu\text{m}$ width was deposited on the $-z$ surface of a congruent LiNbO₃ crystal of 0.5mm thickness. The Ti film was indiffused by heat treatment at 1060°C for 7.5h , to obtain single-mode (at $\lambda\sim 1.55\mu\text{m}$) channel waveguides. Then the unwanted domain-inverted layer induced on the $+z$ surface was removed by polishing to enable the QPM grating formation¹². The QPM grating was then fabricated by two steps: uniform domain inversion over the whole crystal was first made to have the waveguides on the new $+z$ surface, and then a domain-inverted grating was formed by applying a voltage pulse ($\sim 9\text{kV}$) through a periodic electrode.

Generation of cross-polarized twin photons

The basic characteristics of cross-polarized twin

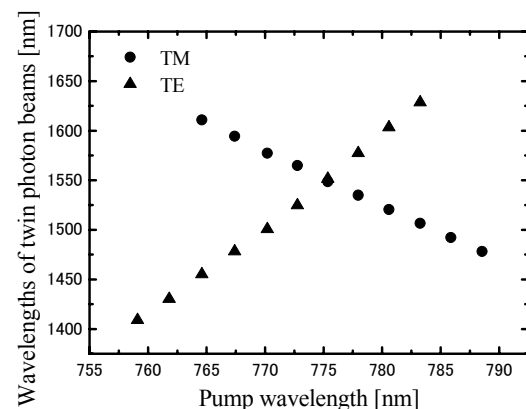


Fig. 2: Measured dependence of the twin-photon wavelengths on the pump wavelength.

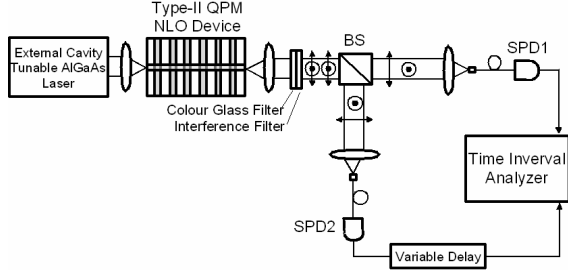


Fig. 3: Setup for measuring the time correlation of the cross-polarized twin photons.

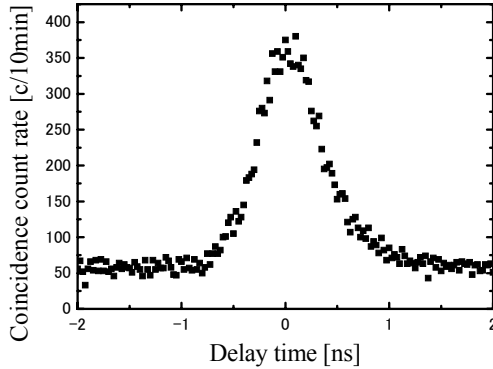


Fig. 4: Correlation of the cross-polarized twin photons.

photon generation were examined by using an external-cavity tunable AlGaAs laser as a pump source. The pump TE mode was excited by end-fire coupling, and the transmitted pump wave was cut by colour-glass and interference filters. Figure 2 shows the dependence of the twin photon wavelengths upon the pump wavelength, measured at room temperature for a typical device of a QPM grating period $\Lambda=9.1\mu\text{m}$. The result agrees well with the prediction^{8,11} calculated by approximating the mode indexes with ordinary and extraordinary indexes of congruent bulk LiNbO₃ crystal. There was an evidence of slight drift of the wavelength-degenerate point due to the photorefractive damage. Therefore, the further experiments were carried out with the device temperature maintained at $90\pm 0.1^\circ\text{C}$. At this temperature, the wavelength-degenerate twin photons of wavelength $\lambda_1=\lambda_2=1559.8\text{nm}$ were generated in a device of a QPM grating period $\Lambda=9.3\mu\text{m}$ pumped at wavelength $\lambda_3=779.9\text{nm}$.

The wavelength bandwidths (FWHM) of the degenerate twin-photons, measured by using a monochromator of 0.9nm resolution, were 1.7nm and 1.8nm for the TE and TM photons, respectively, which were consistent with the theoretical prediction of 1.0nm for both polarizations. The output powers P_1, P_2 of the twin beams, separated by a polarization beam splitter, were measured using InGaAs PIN photodiodes and a lock-in amplifier, and the pump power P_3 was measured at the waveguide output end. The twin photon generation efficiency were $P_1/P_3=1.9\times 10^{-10}$ for TE photons and $P_2/P_3=2.3\times 10^{-10}$

for TM photons, which were of the same order of magnitude as $P_1/P_3=P_2/P_3=5.3\times 10^{-10}$, theoretically predicted⁸ by using the coupling coefficient $\kappa_3=0.12\text{W}^{-1/2}\text{cm}^{-1}$ determined from the result $\eta_{\text{SHG}}=\kappa_3^2 L^2=13\%/W$ of a Type-II QPM second-harmonic generation efficiency measurement.

The time correlation of the generated twin photons was examined by separating the QPM device output into two beams and detecting them by two single photon detectors (SPD's) using Giger-mode InGaAs/InP APDs and analyzing the photon detection signal by using a time interval analyzer (TIA), as shown in Fig.3. The obtained histogram of the coincidence counting rate dependent on the delay time is shown in Fig.4. The result clearly indicates the photon correlation peak at zero delay time with the resolution $\sim 1\text{ns}$ reflecting the jitter of the SPD and the TIA.

Generation of polarization entangled states

Theoretical description:

The wavelength-degenerate twin photon beams generated by the Type-II QPM NLO device can readily be converted into polarization-entangled twin photons by splitting the output beam into two beams by using a beam splitter (BS).

Although the multi-mode-pair model must be used for full description of the state of the twin photons generated by the parametric fluorescence, in the single-mode-pair model the quantum state of the QPM device output may simply be described as⁸

$$|\psi\rangle \approx |0\rangle + r|H,V\rangle, \quad (1)$$

where $|0\rangle$ denotes the vacuum state, and $|H,V\rangle$ the state of twin photons consisting of a horizontally (H) polarized photon and a vertically (V) polarized photon, and r is a constant depending upon the pump power, the device parameters and the deviation from the exact QPM condition. The output twin photon power is calculated by integrating $|r|^2$ over the QPM bandwidth^{8,9}. By omitting the vacuum state term which has no effect on the photon detection and renormalizing the state, the output quantum state can be represented simply by $|H,V\rangle$.

Consider a beam splitter (BS) of a polarization independent power splitting ratio of 1:1. The amplitude operators for the horizontal (x) and vertical (y) components of the fields in the output ports 1 and 2, $a_{1x}, a_{2x}, a_{1y}, a_{2y}$, can be correlated with those for the input ports 1 and 2, $a_{in1x}, a_{in2x}, a_{in1y}, a_{in2y}$, by

$$a_{1x} = \sqrt{1/2} (a_{in1x} + ia_{in2x}), \quad a_{2x} = \sqrt{1/2} (ia_{in1x} + a_{in2x}), \quad (2a)$$

$$a_{1y} = \sqrt{1/2} (a_{in1y} - ia_{in2y}), \quad a_{2y} = \sqrt{1/2} (-ia_{in1y} + a_{in2y}). \quad (2b)$$

The state generated by the QPM-NLO device and fed into the BS input port 1 can be written as

$$|\psi\rangle = |H,V\rangle = a_{in1x}^\dagger a_{in1y}^\dagger |0\rangle, \quad (3)$$

where a_{in1x}^\dagger and a_{in1y}^\dagger are the creation operators. Therefore, the state in the BS output ports is

$$\begin{aligned} |\psi\rangle &= a_{in1x}^\dagger a_{in1y}^\dagger |0\rangle \\ &= (1/2) (a_{1x}^\dagger + ia_{2x}^\dagger) (a_{1y}^\dagger - ia_{2y}^\dagger) |0\rangle \\ &= (1/2) \{ |xy;0\rangle - i|x;y\rangle + i|y;x\rangle + |0;xy\rangle \}. \end{aligned} \quad (4)$$

The states where the cross-polarized twin photon appears together in output port 1 or 2, denoted by $|xy;0\rangle$ and $|0;xy\rangle$, can be omitted since they do not affect the photon coincidence counting. Then after renormalization, we have

$$|\psi\rangle = \sqrt{1/2} \{|x;y\rangle - |y;x\rangle\} \\ = \sqrt{1/2} \{|H;V\rangle - |V;H\rangle\}, \quad (5)$$

where $|x;y\rangle = |H;V\rangle$ denotes the state where a horizontally-(x-)polarized photon appears in the output port 1 and a vertically-(y-)polarized photon appears in the output port 2, and $|y;x\rangle = |V;H\rangle$ the state where a vertically-(y-)polarized photon appears in the output port 1 and a horizontally-(x-)polarized photon appears in the output port 2.

If a polarization-selective phase shifter, which gives a differential phase shift $\Delta\Phi$ to the vertically-polarized component only, is inserted in the output port 1, the output state is given by

$$|\psi\rangle = \sqrt{1/2} \{|H;V\rangle - \exp(i\Delta\Phi)|V;H\rangle\}. \quad (6)$$

Thus the two of the four maximally-entangled Bell states, $|\psi^+\rangle$ and $|\psi^-\rangle$, can be generated by setting as $\Delta\Phi = \pi$ and $\Delta\Phi = 0$ respectively. The time lag between the V and H photons due to the difference in the transit time in the LiNbO₃ waveguide QPM-NLO device can be compensated for by inserting a LiNbO₃ crystal (quantum eraser) of a length $L/2$, corresponding to the half of QPM-NLO device, with the crystallographic orientation 90° rotated with respect to that of the QPM-NLO device^{8,13}.

Generation of the entangled states can be examined by a photon coincidence counting experiment with polarizers inserted with the axis oriented at 45° angle in the two output ports of the BS (see Fig.5). Let XY be coordinate axes rotated 45° with respect to the xy axes (HV axes) for each output port. Then, using the relation between the amplitude operators for the x and y components, and X and Y components, we can rewrite (6) into an expression in XY basis. Omitting the terms which do not affect the coincidence detection, we obtain an expression for the terms which give rise to the coincidence detection through the 45° polarizers

$$|\psi\rangle = (1/2)^{3/2} \{1 - \exp(i\Delta\Phi)\} |X;X\rangle. \quad (7)$$

Therefore, it is expected that, when $\Delta\Phi$ is changed, intensity interference of the photons, characterized by the modulation of the coincidence counting rate in proportion to $|1 - \exp(i\Delta\Phi)|^2$, is observed as a result of the interference of the two terms of the rhs of (6).

Experiment:

Figure 5 shows the experimental setup for the entangled state generation and the photon intensity interference measurement. The output of the QPM-NLO device was split into two beams by a BS. Colour-glass and interference filters were inserted to cut the pump wave, and a tunable filter of 0.9nm FWHM bandwidth was inserted to transmit the wavelength-degenerate twin photons. As the quantum erasers, LiNbO₃ crystals of a length of $L/2 = 15\text{mm}$ were inserted in both output ports of the BS

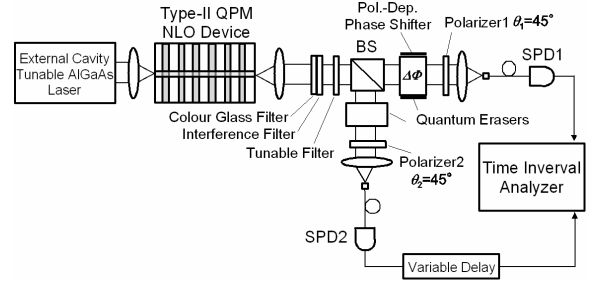


Fig. 5: Setup for polarization entangled state generation and measurement.

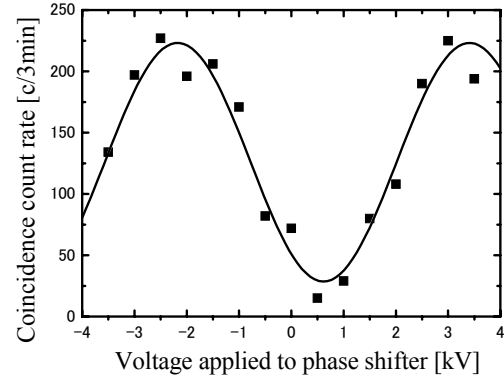


Fig. 6: Experimentally observed photon intensity interference.

with 90°-rotated orientation. Planar electrodes were attached to the z faces of one of the quantum eraser crystals, and DC voltage was applied to them to use the crystal also as an electrooptic polarization-dependent phase shifter for giving $\Delta\Phi$. The half wavelength voltage was $V_\pi = 2.8\text{kV}$. Photon coincidence counting was performed through 45° polarizers for BS outputs by using two SPDs and a TIA. The pump wavelength was carefully adjusted to the wavelength-degenerate point, by monitoring the dependence of the photon counts on the filter tuning.

Figure 6 shows the measured coincidence counting rate (for time window of 2ns) dependent upon the voltage applied to the phase shifter. The accidental coincidence counting rate (smaller than 10% of the maximum coincidence counting rate) was subtracted from the measured rate. Clear periodic modulation in the coincidence counting rate with a period of 5.6kV ($=2V_\pi$), consistent with the theoretical prediction, was observed. The obtained modulation visibility was $V = 0.87$. Similar quantum interference was observed even when the tunable filter of 0.9nm bandwidth was removed, although the visibility slightly degraded to $V \sim 0.6$. These results indicate that the polarization entangled states of (6) were generated.

Entangled photon polarization measurement

It can readily be shown that the polarization entangled state given by (5) is invariant with respect to rotation of the polarization measurement basis.

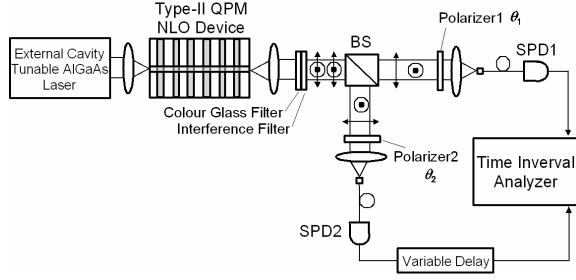


Fig. 7: Setup for twin photon polarization measurement.

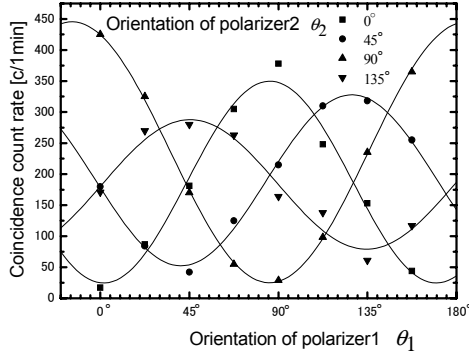


Fig. 8: Coincidence count rate dependent on polarizer orientation.

Let XY be basis axes rotated by an angle θ with respect to the xy (HV) basis axes. Then the invariance can be described as

$$\begin{aligned}
 |\psi\rangle &= \sqrt{1/2} \{|x,y\rangle - |y,x\rangle\} \\
 &= \sqrt{1/2} \{|X,Y\rangle - |Y,X\rangle\}, \quad (8)
 \end{aligned}$$

and it reflects the non-deterministic and non-local nature of the polarizations of entangled photons. Such a nature can be examined by a polarization-selective photon coincident counting experiment. Let θ_1 and θ_2 be the angles of the basis rotation for the output port 1 and 2, respectively. Then a simple theoretical calculation for the state (8) shows that the rate of coincidence counting for X polarized photons in each port is proportional to

$$P_{XX} = \langle \psi | a_{1X}^\dagger a_{2X}^\dagger a_{2X} a_{1X} | \psi \rangle = (1/2) \sin^2(\theta_1 - \theta_2). \quad (9)$$

Figure 7 shows the setup for the polarization-selective photon coincident counting experiment. Polarizers were inserted in front of the two SPDs, and the coincidence counting rate (for time window of 2ns) was measured by using a TIA. Figure 8 shows the measured dependence of the coincidence counting rate on the orientation θ_1 of the polarizer 1 for a few fixed angles θ_2 of the polarizer 2. The result shows the periodic modulations consistent with the theoretical prediction given by (9), although the modulation visibility is not same for different θ_2 . The deviation of the experimental result from (9) would be due to the difference in the detector quantum efficiency and optical coupling efficiency between the output port 1 and 2, and the spurious

reflection at the quantum eraser crystal surfaces. The result, however, clearly demonstrates the non-deterministic and non-local nature of the polarizations of entangled photons, since the result can not be explained by the classic model.

Conclusion

We demonstrated generation of polarization entangled twin photon beams in a simple and efficient system using a Type-II QPM waveguide NLO device. Future work includes solution of the photorefractive-damage problem using MgO:LiNbO₃ crystal, and demonstration of the violation of the Bell's inequality.

Acknowledgments

This work was supported by Grant-In-Aid for Scientific Research on Priority Areas from Ministry of Education, Culture, Sports, Science and Technology (MEXT).

References

- 1 K.Sanaka, K.Kawahara and T.Kuga, Phys. Rev. Lett., vol.86, no.24, pp.5620-5623, 2001.
- 2 S.Tanzilli, W.Tittlel, H.De Riedmatten, H.Zbinden, P. Baldi, M.De Micheli, D.B.Ostrowsky and N.Gisin, Eur. Phys. J. D, vol.18, pp.155-160, 2002.
- 3 T.Suhara, Europ. Conf. Integrated Optics (ECIO'03), Prague, April 1-4, ThP1, pp.73-84, 2003.
- 4 T.Suhara and M.Fujimura, *Waveguide Nonlinear-Optic Devices*, Springer, 2003.
- 5 A.Yoshizawa, R.Kaji and H.Tsuchida, Electron. Lett., vol.39, no.7, pp.621-622, 2003.
- 6 S.Tanzilli, W.Tittel, M.Halder, O.Alibert, P.Baldi, N.Gisin and H.Zbinden, Nature, 437, pp.116-120, 2005.
- 7 D.Bouwmeester, A.Ekert, and A.Zeilinger, Eds., *The Physics of Quantum Information*. Springer, 2000.
- 8 T.Suhara and H.Kintaka, IEEE J. Quantum Electron., vol.41, pp.1203-1212, 2005.
- 9 T.Suhara and T.Nosaka, IEEE J. Quantum Electron., vol.42, pp.777-784, 2006.
- 10 H.Kintaka and T.Suhara, Jpn. J. Appl. Phys., vol.43, no.5A, pp.2545-2546, 2004.
- 11 T.Nosaka, B.K.Das, M.Fujimura and T.Suhara, IEEE Photon. Tech. Lett., vol.18, pp.124-126, 2006.
- 12 D.Hofmann, G.Schreiber, C.Haase, H.Herman, W.Grundkotter, R.Rcken and W.Sohler, Opt. Lett., vol.24, no.13, pp.896-898, 1999.
- 13 Y.Shih, IEEE J. Selected Topics Quantum Electron., vol.9, no.6, pp.1455-1467, 2003.